Hindawi
Advances in Materials Science and Engineering
Volume 2020, Article ID 1384194, 12 pages
https://doi.org/10.1155/2020/1384194

Research Article

Research on Recovery Mechanism and Process of Waste Thermosetting Phenolic Resins Based on Mechanochemical Method

Jian Hu,[1] Huifang Dong ,[1] and Shouxu Song [2]

[1]*School of Mechanical Engineering, Chaohu University, Chaohu, Anhui, China*
[2]*Key Laboratory of Green Design and Manufacturing in Mechanical Industry, Hefei University of Technology, Hefei, Anhui, China*

Correspondence should be addressed to Huifang Dong; 253984415@qq.com

Received 31 December 2019; Accepted 24 February 2020; Published 19 March 2020

Academic Editor: Francisco Javier Fernández Fernández

The present study analyzed the recovery mechanism of the thermosetting phenolic resin waste, optimizing the recovery process parameters, based on the mechanochemical recovery method. The physical and chemical structure of the ultrapulverized phenolic resin powder was characterized by the low-field NMR (nuclear magnetic resonance), IR (infrared spectroscopy), and SEM (scanning electron microscopy). The recovery process parameters were designed by using the response surface analysis method, and the multiple quadratic regression model was established and the multiobjective process parameter was optimized. The results show that the body network structure of the material is destroyed during the crushing process. The intensity of the internal cross-linking signal is reduced and tends to be stable at about 60%, when the particle size exceeds 120 mesh. The cross-linking bonds methylene (-CH_2-) in the main chain of the molecular chain and the C-O bond in the methylol group on the branch are broken. The tensile strength of the recycled sheet made of the phenolic resin powder is 8.27 MPa, and the bending strength is 17.76 Mpa through the mechanical properties test. The influences on the change rate of the cross-linking signal intensity and the yield of the recycled powder are in the following order: rotation speed, feed size, time, and feed volume. The best recovery parameters are as follows: rotation speed of 2820 r/min, time of 80 min, feed particle diameter of 0.43 mm, and feed volume of 60 g.

1. Introduction

Thermosetting phenolic resins are widely used in construction, transportation, mining, and other industries due to their excellent performance of heat resistance, corrosion resistance, and adhesive strength. However, due to their thermosetting characteristics, thermosetting phenolic resins cannot be remelted or dissolved in solvents after curing and setting [1], which are extremely difficult to be recycled. There are 3 ways to recycle waste thermosetting plastics: physical recycling method, chemical recycling method, and heat recycling method. For physical recycling, the value of recycled materials is low, even the process is simple and the cost is low. After recycling, the high-value thermosetting plastics become low-value products, such as plastic fillers and concrete aggregates [2–6]. The chemical recycling method is difficult to be industrialized, because of expensive equipment, complicated processes, and high recovery costs [7–11]. The recovery and utilization rate of heat recycling is low, which generates toxic organic gases during the processing, causing environmental secondary pollution [12].

If the high-value and low cost resource method of thermosetting plastic with high efficiency can be found, which will save resources and energy, reduce pressure on environmental pollution, and provide high cost-effective materials for lightweight design, the mechanochemical method [13–15] changes its physical and chemical properties and molecular structure of the substance, improves its reactivity through the accumulation of mechanical energy caused by the action of mechanical force, and induces

chemical reactions which are difficult or impossible to be performed by using thermochemistry. For example, the study on the lead mechanochemical sulfidation of fluorescent tube core glass under mechanical force [16] and the study on the surface modification of MSWI (municipal solid waste incineration) fly ash used the mechanochemical method and mixed it with polypropylene to form a composite material [17].

However, there are few studies on the mechanochemical recovery of thermosetting phenolic resins. In particular, the present studies lack research on the change law of molecular structure of thermosetting phenolic resin under mechanical force, the mechanochemical changes that occur during the recovery process, and the relationship between the physical and chemical properties of the recycled materials and the process parameters. To deal with these problems, and in order to provide the theoretical foundation and experimental basis for the recovery of the waste thermosetting phenolic resins with high efficiency and high-value, the recovery mechanism of thermosetting phenolic resin under the action of mechanical force was studied and the recovery process was optimized in the present study.

2. Mechanochemical Recovery Method of Thermosetting Phenolic Resin

The occurrence of critical stress made by unevenly distributed internal stress or impact energy concentrates on individual segments under the combined action of a variety of strong mechanical forces (grinding, compression, impact, shear, extension, etc.) during the process of high-speed pulverization of thermosetting phenolic resin and causes the chemical bond to be broken. Moreover, the thermal energy generated by the mechanical force facilitates the breaking of the weak chemical bond in the molecular structure, which destroys the highly cross-linking network structure of the thermosetting phenolic resin, enhances the activity of the functional group, and reduces the degree of cross-linking. The material recovers plasticity at a certain degree and the ability to be processed and formed again because of the low-cross-linking high polymer is produced during the above processing, which achieves the thermosetting phenolic resin recovery.

The recovery process of the mechanochemistry method for the thermosetting phenolic resin is shown in Figure 1.

2.1. Laboratory Equipment. The experiment was carried out on a self-made experimental machine at room temperature. The crushing cavity of the experimental machine is divided into a shearing cavity composed of a shear arbor 7 and a fixed annular cutter 8, and a grinding cavity composed of a static grinding disc 3 and a moving grinding disc 4. The two-dimensional diagram of the experimental machine mechanism and the three-dimensional model of the grinding cavity tool are shown in Figure 2. The main technical parameters of the experimental machine: ① Motor speed range: 500~7000 r/min; ② The maximum output torque of the motor: 15 Nm; ③ The maximum feed weight is 150 g.

The experimental equipment works as follows: the thermosetting phenolic resin particles become smaller size particles under the action of strong shear and impact between the high-speed rotating shearing arbor 7 and the teeth of the annular cutter 8, when it enters the shearing cavity from the feed inlet 2. The smaller particles enter the grinding cavity under the combined effect of the flow field inside the cavity and the centrifugal force and are subjected to strong vertical and circumferential shear, a variety of mechanical forces such as extrusion, friction, and the further effect of the temperature field, which are fully crushed, dispersed, mixed, and causes mechanochemical reaction to achieve its degradation and regeneration.

2.2. Experimental Procedure. First, the thermosetting phenolic resin from waste wall external insulation board (produced by China Commercial Insulation Materials (Langfang) Co., Ltd.) was washed and dried and put into a composite crusher for coarse crushing. The particles obtained by the coarse crushing are as shown in Figure 3. Second, the coarse crushing particles were collected and put into the self-made recovery machine for ultrafine crushing. The speed of the experimental machine was adjusted to 2000–3000 r/min, the feeding amount was 50–70 g, and the feeding particle size was 0.4–1.5 mm. The test was designed for 60 min–120 min, and the phenolic resin powder is shown in Figure 3. There was no obvious oxidation and agglomeration phenomenon, and the powders had high activity, which can cause obvious plastic deformation under the action of extrusion stress. The phenolic resin powder with 120 mesh was sieved by a vibrating screen and collected and mixed with polyvinyl chloride at a ratio of 8 : 2; then the experimental slat samples were made by means of moulding pressing technology as shown in Figure 4. The average tensile strength is 8.13 MPa, and the average bending strength is 17.65 Mpa, tested on the MTS-809 hydraulic servo material testing machine, which means that samples have good comprehensive mechanical properties.

3. Analysis of Recovery Mechanism

3.1. Test Analysis

3.1.1. NMR (Nuclear Magnetic Resonance) Analysis. The formula for the decay process of magnetization with time (t) during the relaxation process is shown as follows [18]:

$$M(t) = A \cdot \exp\left(-\frac{t}{T_{21}} - \frac{1}{2}qM_{r1} \cdot t^2\right) + B \cdot \exp\left(-\frac{t}{T_{21}}\right) + C \cdot \exp\left(\frac{t}{T_{22}}\right) + D, \quad (1)$$

where A is the ratio of the internal cross-linked chain signal to the total signal; T_{21} is the relaxation time of the internal cross-linked chain signal and the catenary chain signal; q is interelectrode interaction. When the temperature is much higher than the glassy temperature, q value is ignored. M_{r1} is

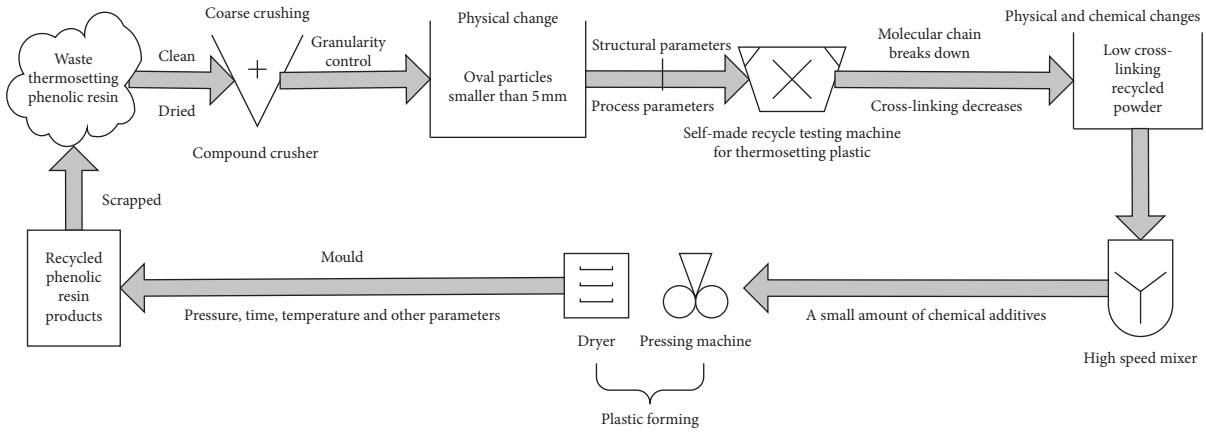

Figure 1: Closed-loop recovery process of thermosetting phenolic resin.

dipole moment in the rigid lattice molecule; B is the proportion of the signal of the overhang chain to the total signal; C is the proportion of the sol signal to the total signal; T_{22} is the relaxation time of the sol signal; D is DC (direct current) component used in analysis, which has no practical physical meaning.

The parameters in formula (1) for phenolic resin materials and its regenerated powders with different particle sizes (60 mesh, 80 mesh, 120 mesh, 160 mesh, and 200 mesh) were measured by using a nuclear magnetic resonance cross-link density analyzer (MicroMR-CL, Shanghai Newmax Technology Corporation). The change law of the degree of cross-linking was analyzed, as labeled in Figure 5.

The parameters for the NMR test are given in Table 1.

The intensity of the cross-linking signal inside phenolic resin material is significantly reduced after pulverization, which indicates that the cross-linking bonds are broken. The decrosslinking effect of the phenolic resin material increased with decreasing particle size. The cross-linking signal intensity tends to be stable at about 60% when the particle size exceeds 120 mesh.

3.1.2. IR (Infrared Spectrum) Analysis. The regenerated powder of phenolic resin was wrapped in a Soxhlet extractor with filter paper and extracted with acetone as a solvent for 24 hours to remove small molecular impurities such as additives, and then dried and extracted with xylene as a solvent for 24 hours to obtain sol extract. Sol extract was covered on a KBr tablet for IR analysis by using an infrared spectrometer (Nicolet 67, Thermo Nicolet, USA).

IR of phenolic resin recycled powder with different particle sizes in Figure 6 shows that the stretching vibration of the methylene (-CH_2-) at 2908 cm^{-1} is enhanced significantly and shifted to 2920 cm^{-1}, while the absorption peak of the methyl (-CH_3) at 1439 cm^{-1} is increased significantly, which indicates that the methylene (-CH_2-) on the main chain of the phenolic resin is cleaved to form a methyl group (-CH_3), and the fracture of the methylene (-CH_2-) is not caused by thermal oxidation because the carbonyl group (C=O) and carboxyl group (COOH) do not show up. The absorption peak of the hydroxyl group (-OH) at 3361 cm^{-1} is increased, and the stretching vibration of a methylol C-O bond at 1061 cm^{-1} is increased, indicating that the hydroxymethyl C-O bond in the branch is broken to generate hydroxyl radical (OH).

3.1.3. SEM (Scanning Electron Microscope) Analysis. To analyze the microstructure and morphological of the phenolic resin material, the phenolic resin and recycled powder were tested by using a scanning electron microscope (JSM-6490LV, manufactured by Japan Electronics).

Figure 7 shows the cross-sectional micrographs of the thermosetting phenolic resin before and after crushing with 200 mesh. The densely spaced network structure of the thermosetting phenolic resin is highly cross-linked, which is destroyed under the action of strong mechanical forces, the phenolic resin matrix is broken into strands, and the surface of the powder is rough and cotton-wool shaped.

3.1.4. Elementary Analysis. To analyze the change law before and after crushing, the element content of the thermosetting phenolic resin material and phenolic resin powder tested by using the elemental analyzer (Vario EL III, Elementar, Germany) are shown in Figure 8. The content does not show any change before and after pulverization, such as carbon, hydrogen, and oxygen, which indicates that the elements of carbon, hydrogen, and oxygen are not separated from the material when methylene (-CH_2-) and methylol (C-O) in the cross-linking structure of phenolic resin are destroyed.

3.2. Mechanochemical Model for Decrosslinking of Thermosetting Phenolic Resin. A mechanochemical model for the thermosetting phenolic resin to delink under mechanical force was established based on the above analysis, as shown in Figure 9.

The molecular chain model of the thermosetting phenolic resin network cross-linking structure is shown in Figure 9(a). The stress field generated by the strong mechanical force acts on the molecular chain of the phenolic resin. The internal stress is distributed randomly. The molecular chain with stress concentration is broken to generate

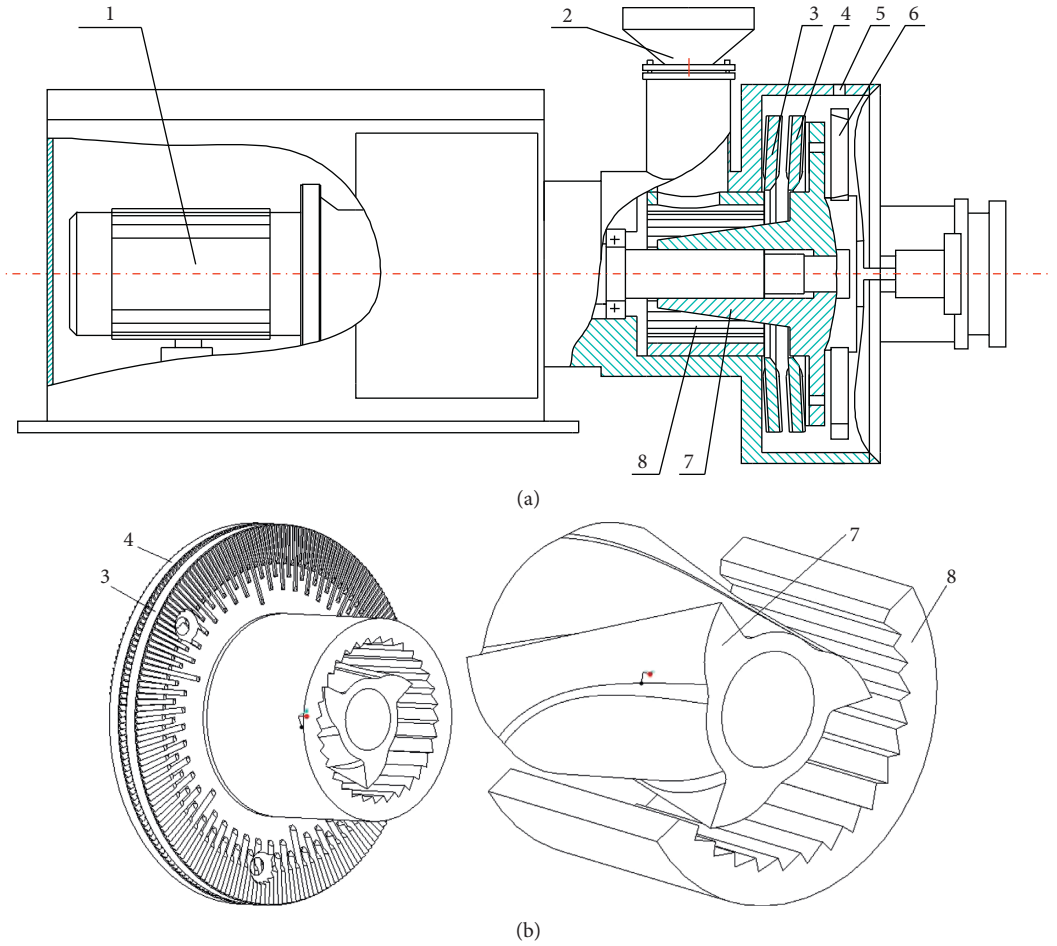

Figure 2: Model of experimental machine. 1: stepless speed regulating motor; 2: feed inlet; 3: static grinding disc; 4: moving grinding disc; 5: temperature sensor; 6: impeller-type stirring cutter; 7: shearing arbor; 8: fixed annular cutter. (a) Schematic diagram of thermosetting plastic recovery experimental machine. (b) Three-dimensional model of the crushing cavity.

Figure 3: Phenolic resin powder.

Figure 4: Phenolic resin recycled slat samples.

a terminal active group (-CH_2 ●) and a hydroxyl radical (OH), which is shown in Figure 9(b) because the bond energy of the cross-linking C-C bond and the C-O bond on the hydroxymethyl group in the branch chain is weak. These terminal groups and radicals which have high activity, contact with each other, or with the internal groups in the cross-linking structure to activate the reaction to generate stable terminal groups (-CH_3 and -OH), as shown in Figure 9(c). The broken number of cross-link bonds is increased with the continuous action of mechanical force, which leads to the network cross-linking structure of the phenolic resin that is damaged to a certain extent and generates linear small molecular chains, as shown in Figure 9(d).

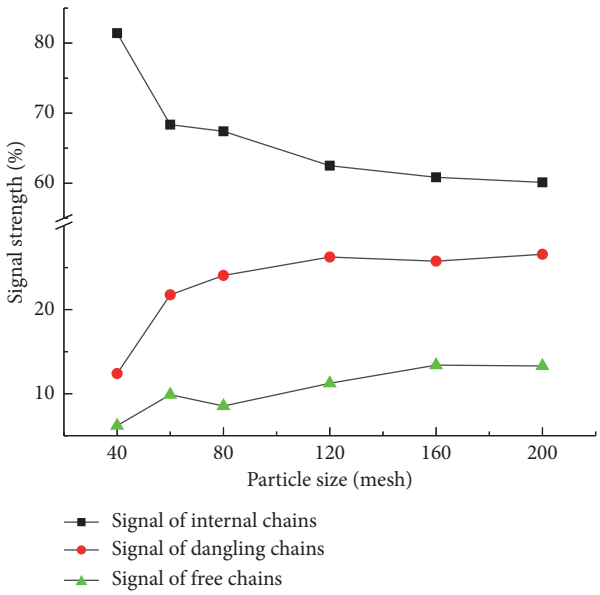

Figure 5: Changes in the cross-linking degree of phenolic resin before and after pulverization.

Table 1: The parameters of the NMR test.

Resonance frequency	Magnet strength	Coil diameter	Temperature
21.8 MHz	0.52 T	10 mm	180°C

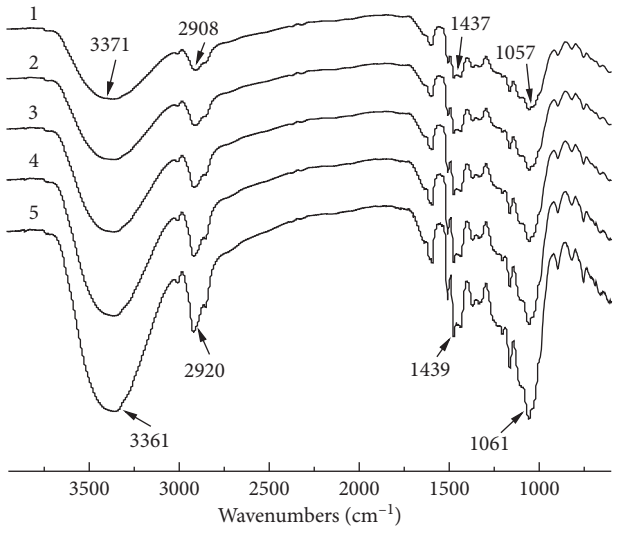

Figure 6: IR of the phenolic resin recycled powder with different particle sizes. 1, 2, 3, 4, 5: particle size of 60 mesh, 80 mesh, 120 mesh, 160 mesh, 200 mesh.

4. Research on Recovery Process of Thermosetting Phenolic Resin

4.1. Evaluation Index of Thermosetting Phenolic Resin Recovery Effect. According to the test and analysis results of the degree of cross-linking and IR of the recycled phenolic resin powder, it can be concluded that the methylene (-CH_2-) in its main chain and the hydroxymethyl C-O bond on the branched chain are broken obviously under the action of mechanical force, during the crushing process of phenolic resin. With the decrease of particle size, the cross-linking signal intensity is stabilized when the particle size is more than 120 meshes. Therefore, the change rate of the cross-linking signal intensity and the yield of the recycled powder were taken as two indicators for evaluating the recovery effect of the thermosetting phenolic resin.

The definition of the evaluation index of the thermosetting phenolic resin recovery effect is as follows.

4.1.1. Determination of the Change Rate of Cross-Linking Signal Intensity. The ratio of the signal of the cross-linked chain portion of the phenolic resin material to the total signal A_1 was tested; the recycled powder of the phenolic resin in the crushing cavity was collected, and the ratio of the signal of the cross-linked chain portion of the regenerated powder to the total signal A_2 was tested. The formula for calculating the change rate of cross-link signal intensity Y_1 is shown as follows:

$$Y_1 = \left(1 - \frac{A_2}{A_1}\right) \times 100\%. \quad (2)$$

4.1.2. Determination of Yield of Recycled Powder. The mass m_1 (g) of the phenolic resin material before crushing was tested; the phenolic resin recycled powder in the crushing cavity after crushing was collected and sieved with a 120 mesh screen; the mass m_2 (g) of the recycled powder with a particle size smaller than 120 mesh was measured. The formula for calculating the yield Y_2 of the 120-mesh phenolic resin regeneration powder is shown in the following formula:

$$Y_2 = \frac{m_2}{m_1} \times 100\%. \quad (3)$$

4.2. Experimental Design. According to the Box-Behnken design method [19, 20], the four important factors of speed, time, feed size, and feed volume were selected as independent variables (represented with X_1, X_2, X_3, and X_4, respectively), and the range was determined according to the existing experimental conditions and research experience. The rotation speed was 2000–3000 r/min, the time was 60–120 min, the feed particle diameter was 0.425–1.275 mm, and the feed volume was 50–70 g. Each factor was taken in 3 levels and encoded according to the equation $x_i = (X_i - X_{i0})/\Delta X_i$ (x_i is the encoding value of the independent variable; X_i is the true value of the independent variable, where $i = 1, 2, 3, 4$; X_{i0} is the true value of the independent variable at the center of the experiment; ΔX_i is the independent variable step size). The change rate of the cross-linking signal intensity Y_1 and the yield of recycled powder Y_2 were used as the response values, 29 experimental points were designed for response surface analysis experiments, of which 24 experimental points were factorial points and 5

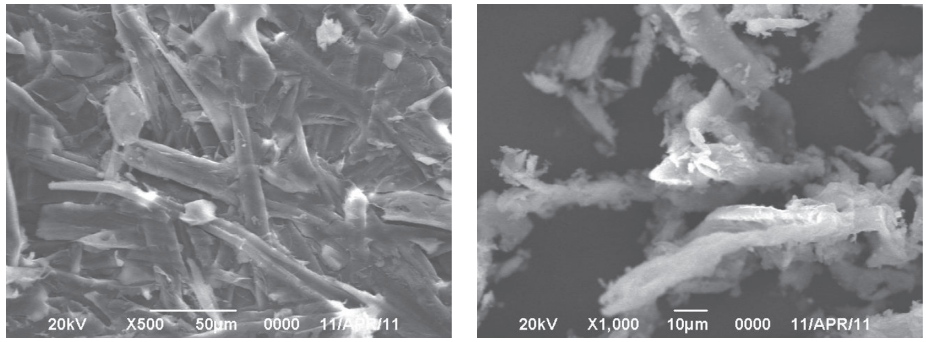

(a) (b)

Figure 7: Surface morphology of phenolic resin before and after crushing. (a) Phenolic resin raw material (×500 times). (b) Phenolic resin powder with 200 mesh (×1000 times).

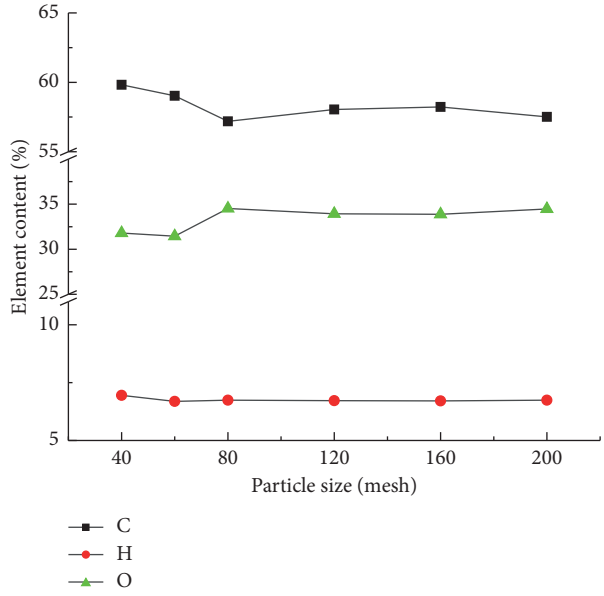

Figure 8: Element content changes of phenolic resin before and after crushing.

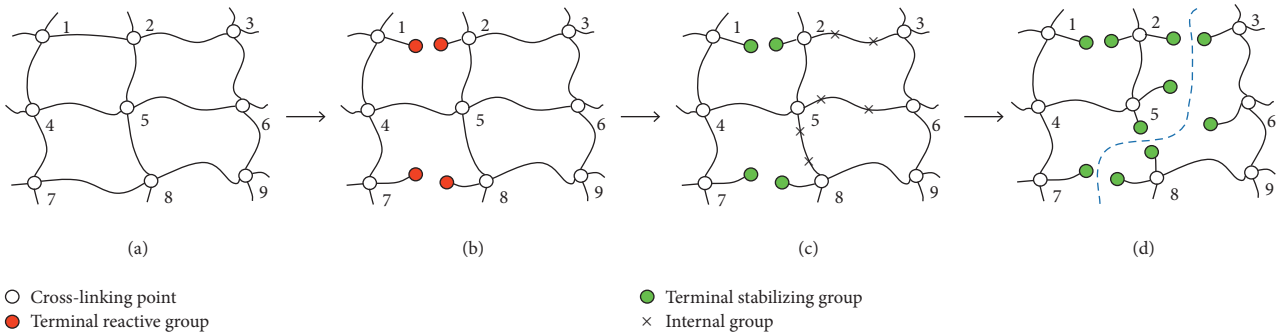

Figure 9: Mechanochemical model for decrosslinking of the thermosetting phenolic resin.

experimental points were zero points used to estimate experimental error. The coding and level of the experimental independent variable factor are shown in Table 2. The experimental design and response values are shown in Table 3.

4.3. Analysis of Experimental Results. A quadratic multiple regression fit was performed with data in Table 4 by using Design-Expert 8.0.6 software, and the regression equation is as follows:

Table 2: Coding and level of the experimental independent variable factor.

Factor	Coding value (x_i) and level of the independent variable		
	−1	0	1
X_1 speed (r/min)	2000	2500	3000
X_2 time (min)	60	90	120
X_3 feed size (mm)	0.425	0.85	1.275
X_4 feed volume (g)	50	60	70

Table 3: Experimental design and response value.

Experiment number	Factor				Response value	
	x_1	x_2	x_3	x_4	Y_1 (%)	Y_2 (%)
1	−1	−1	0	0	24.793	56.417
2	1	−1	0	0	31.357	85.433
3	−1	1	0	0	28.336	68.576
4	1	1	0	0	32.128	88.913
5	0	0	−1	−1	32.341	85.341
6	0	0	1	−1	28.853	71.129
7	0	0	−1	1	32.805	87.593
8	0	0	1	1	29.924	75.615
9	−1	0	0	−1	26.015	60.584
10	1	0	0	−1	32.121	88.396
11	−1	0	0	1	27.878	67.658
12	1	0	0	1	32.413	89.619
13	0	−1	−1	0	31.979	83.414
14	0	1	−1	0	31.983	83.823
15	0	−1	1	0	26.692	63.258
16	0	1	1	0	30.712	78.731
17	−1	0	−1	0	29.371	73.118
18	1	0	−1	0	32.641	90.894
19	−1	0	1	0	23.338	51.346
20	1	0	1	0	31.264	84.745
21	0	−1	0	−1	30.133	76.593
22	0	1	0	−1	30.346	77.235
23	0	−1	0	1	30.315	77.176
24	0	1	0	1	30.392	77.336
25	0	0	0	0	31.149	80.631
26	0	0	0	0	32.137	84.256
27	0	0	0	0	31.987	84.138
28	0	0	0	0	32.306	84.103
29	0	0	0	0	32.074	84.172

$$\begin{aligned} Y_1 = {} & 31.93 + 2.68x_1 + 0.72x_2 - 1.7x_3 + 0.33x_4 \\ & - 0.69x_1x_2 + 1.16x_1x_3 - 0.39x_1x_4 \\ & + x_2x_3 - 0.034x_2x_4 + 0.15x_3x_4 - 1.93x_1^2 \\ & - 0.99x_2^2 - 0.65x_3^2 - 0.44x_4^2, \end{aligned} \tag{4}$$

$$\begin{aligned} Y_2 = {} & 83.46 + 12.53x_1 + 2.69x_2 - 6.61x_3 + 1.31x_4 \\ & - 2.17x_1x_2 + 3.91x_1x_3 - 1.46x_1x_4 \\ & + 3.77x_2x_3 - 0.12x_2x_4 + 0.56x_3x_4 - 5.31x_1^2 \\ & - 3.91x_2^2 - 2.39x_3^2 - 1.73x_4^2. \end{aligned} \tag{5}$$

Reliability analysis of regression models (4) and (5) was performed, which is shown in Table 4. The variance analysis results of regression models are shown in Table 5.

Table 4: Reliability analysis of regression models.

Response	Fitness	Adjusted R Square	Precision	Significance level (P value)	
				Model	Lack of fit
Y_1	0.9734	0.9468	21.637	<0.0001	0.2928
Y_2	0.9785	0.9569	24.888	<0.0001	0.2388

The significance levels of the models of Y_1 and Y_2 are less than 0.01 from the data analysis in Table 4, which indicates that the regression model is highly significant, and the significance levels of the lack of fit are greater than 0.05, which indicates that the regression model has a high degree of fit. The adjusted R square of the models of Y_1 and Y_2 are all greater than 0.8, and the fitness of Y_1 and Y_2 model are 0.9734 and 0.9785, which indicates that the regression model has good fitness. In this experiment, 97.34% and 97.85% of the data were used for Y_1 and Y_2 regression models. In order to make the regression model have higher reliability, the precision is generally required to be greater than 4. Therefore, the fitted regression models of Y_1 and Y_2 have high reliability and can be used to optimize the process parameters for the crushing and regeneration of the thermosetting phenolic resin.

The analysis for the data in Table 5 indicates that in the Y_1 model for the change rate of the cross-linking signal intensity, the primary terms x_1 ($P < 0.0001$), x_2 ($P = 0.0007$), and x_3 ($P < 0.0001$), interaction terms $x_1\,x_3$ ($P = 0.0012$) and $x_2\,x_3$ ($P = 0.0034$), and quadratic terms x_1^2 ($P < 0.0001$) and x_2^2 ($P = 0.0006$) are significant extremely, interaction terms $x_1\,x_2$ ($P = 0.0294$) and quadratic terms x_3^2 ($P = 0.0116$) are significant, and the remaining terms are not significant; in the Y_2 model for the yield of recycled powder, the primary terms x_1 ($P < 0.0001$), x_2 ($P = 0.0006$), and x_3 ($P < 0.0001$), interaction terms $x_1\,x_3$ ($P = 0.0026$) and $x_2\,x_3$ ($P = 0.0034$), and quadratic terms x_1^2 ($P < 0.0001$) and x_2^2 ($P = 0.0004$) are extremely significant; the quadratic term x_3^2 ($P = 0.0128$) is significant, and the remaining terms are not significant. The influence on the change rate of the cross-linking signal intensity is in order: speed, feed size, time, and feed volume; the influence on the yield of recycled powder is in order: speed, feed size, time, and feed volume.

The response surface diagrams of the interaction between the factors X_1, X_2, X_3, and X_4 on the response values Y_1 and Y_2 are shown in Figure 10 and Figure 11, respectively. In general, the higher the rotation speed, the smaller the particle size of the feed, and the longer the pulverization time, the greater the change rate of the cross-linking signal intensity, and the higher the yield of the recycled powder, whereas the effect of feed volume on them is not significant. The higher the rotation speed, the greater the intensity of the stress field in the crushing cavity, and the greater the mechanical energy per unit volume of particles accumulates. The smaller the particle size of the feed, the more the number of particles in the crushing cavity, the higher the frequency of particle impact, then the regular impact promotes the rapid accumulation of mechanical energy. The longer the pulverization time, the longer the acting time of the stress field and the faster the mechanical energy is accumulated. The internal stress generated by the continuous action

Table 5: Variance analysis of regression models.

Source of variance	Change rate of the cross-linking signal intensity Y_1				Yield of the recycled powder Y_2			
	Sum of squares	Degree of freedom	F value	Significance level (P value)	Sum of squares	Degree of freedom	F value	Significance level (P value)
x_1	86.27	1	264.01	<0.0001**	1882.53	1	411.66	<0.0001**
x_2	6.2	1	18.98	0.0007**	87.06	1	19.04	0.0006**
x_3	34.53	1	105.66	<0.0001**	524.82	1	114.76	<0.0001**
x_4	1.28	1	3.91	0.0679	20.59	1	4.5	0.0522
$x_1\ x_2$	1.92	1	5.88	0.0294*	18.83	1	4.12	0.0619
$x_1\ x_3$	5.38	1	16.46	0.0012**	61.02	1	13.34	0.0026**
$x_1\ x_4$	0.62	1	1.89	0.191	8.56	1	1.87	0.1929
$x_2\ x_3$	4.03	1	12.34	0.0034**	56.73	1	12.41	0.0034**
$x_2\ x_4$	$4.62E-3$	1	0.014	0.907	0.058	1	0.013	0.9119
$x_3\ x_4$	0.092	1	0.28	0.6038	1.25	1	0.27	0.6096
x_1^2	24.21	1	74.10	<0.0001**	182.68	1	39.95	<0.0001**
x_2^2	6.37	1	19.49	0.0006**	98.97	1	21.64	0.0004**
x_3^2	2.75	1	8.41	0.0116*	37.16	1	8.13	0.0128*
x_4^2	1.28	1	3.92	0.0676	19.52	1	4.27	0.0578

*Significant difference ($P < 0.05$); **extremely significant difference ($P < 0.01$).

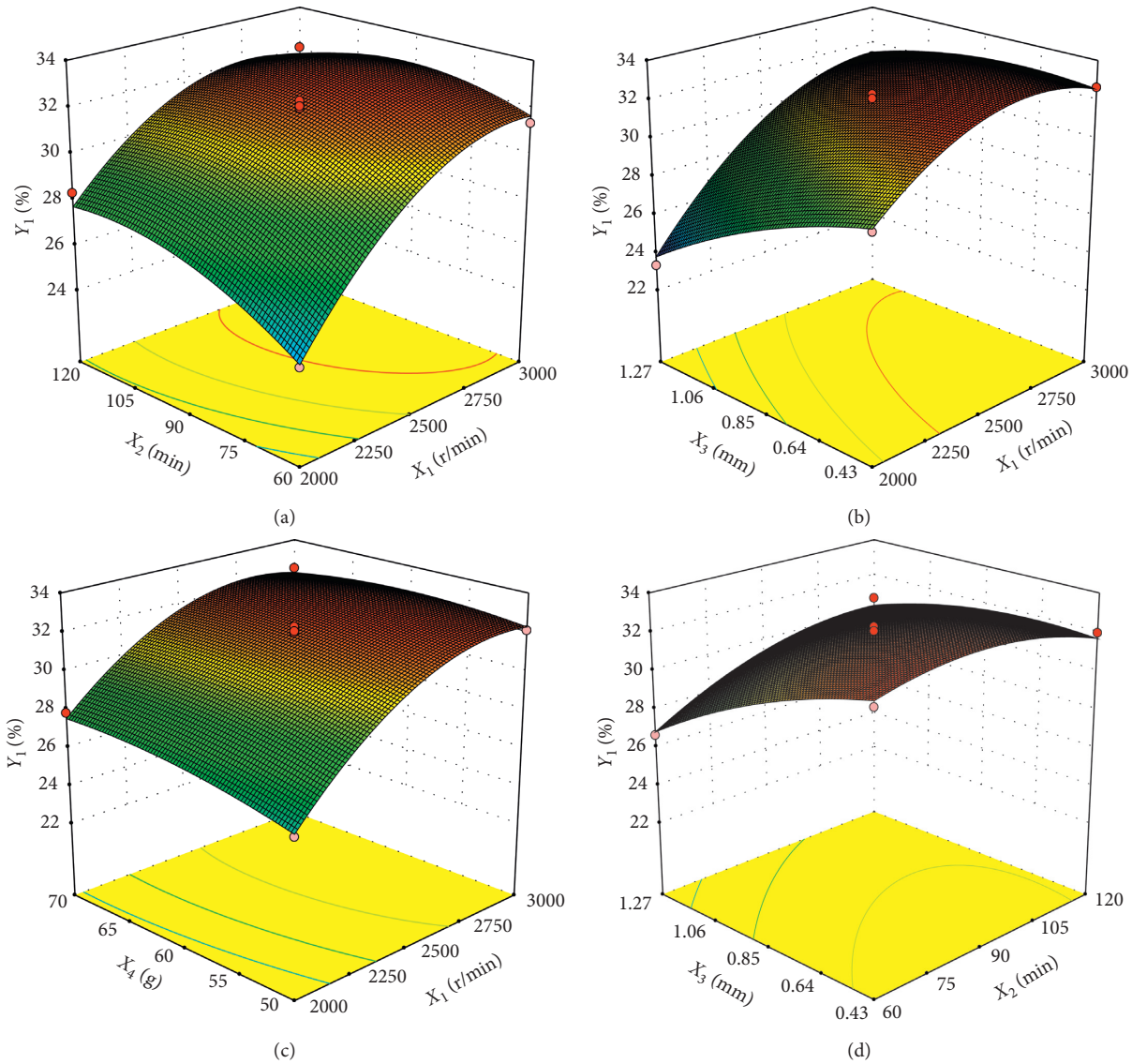

Figure 10: Continued.

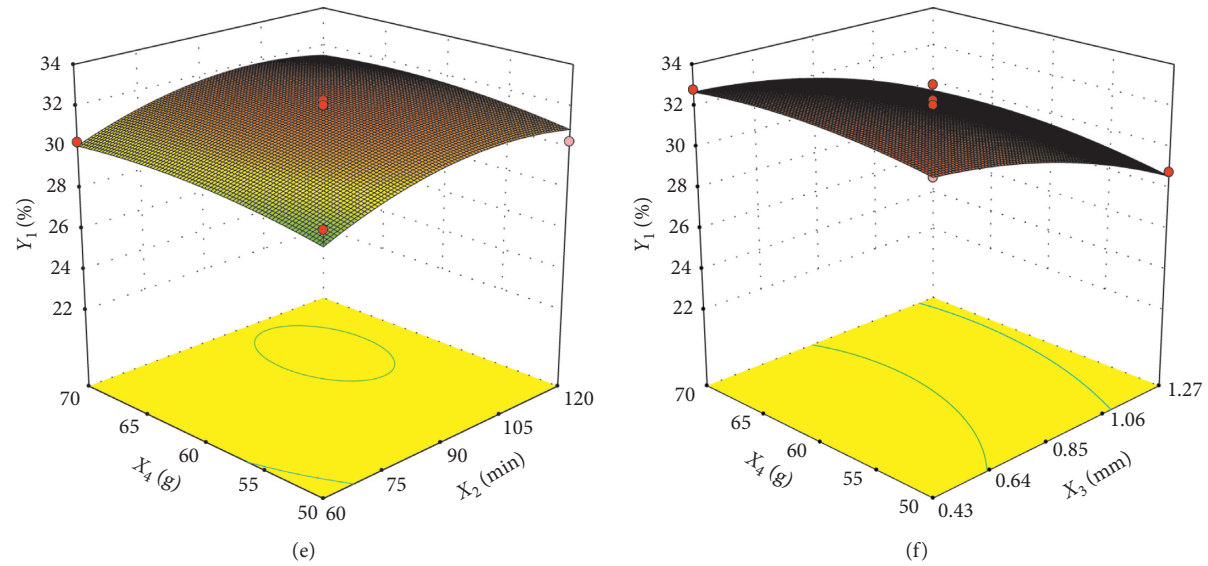

Figure 10: Effect of interaction factors on the change rate of the cross-linking signal intensity. (a) $X_3 = 0.85$ mm, $X_4 = 60$ g. (b) $X_2 = 90$ min, $X_4 = 60$ g. (c) $X_2 = 90$ min, $X_3 = 0.85$ mm. (d) $X_1 = 2500$ r/min, $X_4 = 60$ g. (e) $X_1 = 2500$ r/min, $X_3 = 0.85$ mm. (f) $X_1 = 2500$ r/min, $X_2 = 90$ min.

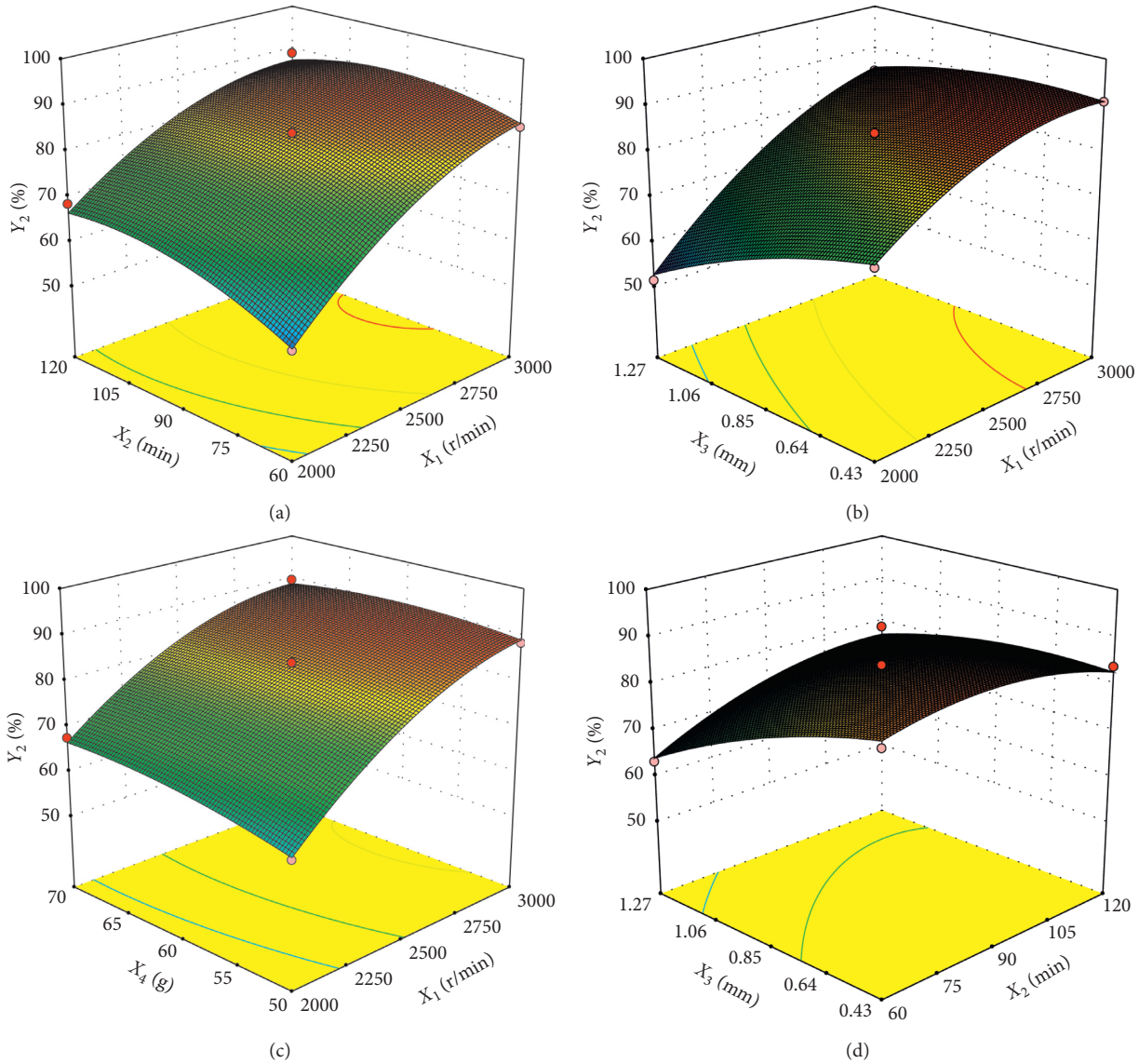

Figure 11: Continued.

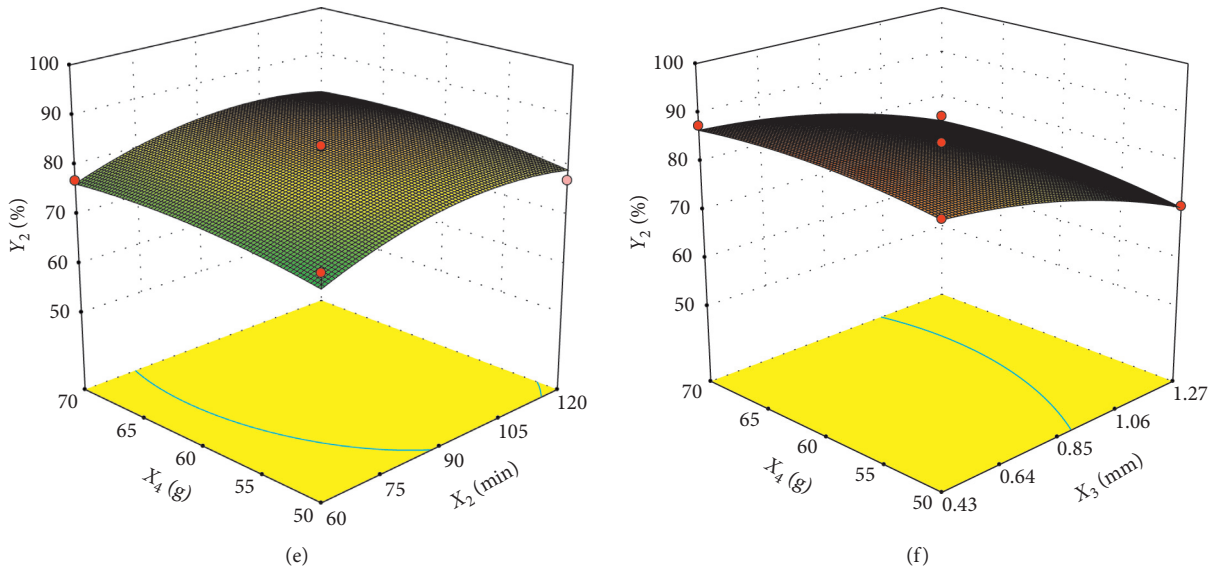

Figure 11: Effect of interaction factors on the yield of 120 mesh phenolic resin powder. (a) $X_3 = 0.85$ mm, $X_4 = 60$ g. (b) $X_2 = 90$ min, $X_4 = 60$ g. (c) $X_2 = 90$ min, $X_3 = 0.85$ mm. (d) $X_1 = 2500$ r/min, $X_4 = 60$ g. (e) $X_1 = 2500$ r/min, $X_3 = 0.85$ mm. (f) $X_1 = 2500$ r/min, $X_2 = 90$ min.

of mechanical energy promotes the breaking of weak cross-links in the molecular structure of the phenolic resin and results in breaking inside the particles, expansion, and eventually fracture. With the breaking of the cross-linking bond and the decrease of the particle size, the fine powder flows to the edge area of the stress field and then leaves the stress field area. Although the strength of the stress field increases and the duration is prolonged, the effective strength of the stress field received by the fine powder does not increase, and the duration is reduced. At this time, the cleavage of the cross-linking bond in the molecular chain of the phenolic resin is restricted.

4.4. Parameter Optimization and Verification. In order to obtain the optimal process parameters of the thermosetting phenolic resin for pulverization and regeneration, it is necessary to perform multiobjective optimization of the change rate of cross-linking signal intensity and the yield of regeneration powder for each parameter. According to the actual working conditions and the analysis results of the regression model, the constraints for the optimization analysis are set as follows:

$$\begin{cases} \max Y_1(X_1, X_2, X_3, X_4), \\ \max Y_2(X_1, X_2, X_3, X_4), \end{cases}$$

$$\text{s.t.} \begin{cases} -1 \le X_1 \le 1, \\ -1 \le X_2 \le 1, \\ -1 \le X_3 \le 1, \\ -1 \le X_4 \le 1. \end{cases} \quad (6)$$

The optimized response surface is shown in Figure 12. In the response surface, the optimal expected value is 0.554515;

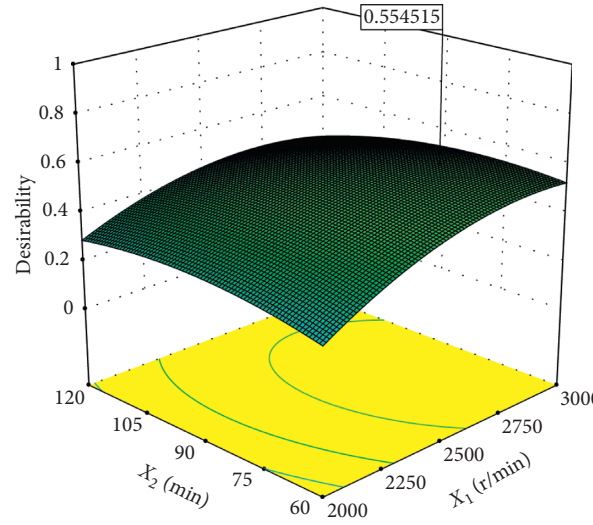

Figure 12: Response surface of optimization results.

when the rotation speed is 2817.23 r/min, the time is 79.8 min, the diameter of the feeding particle is 0.43 mm, and the feeding volume is 59.44 g. The change rate of the cross-linking signal intensity is 33.298%, and the yield of the recycled powder is 91.396%.

In order to facilitate the practical operation, the theoretical value of the optimization parameter is rounded as follows: rotation speed is 2820 r/min, time is 80 min, the feeding particle diameter is 0.43 mm, and the feeding volume is 60 g. The predicted values of the change rate of the cross-linking signal intensity are 33.293% and 91.411%, respectively. The results are shown in Table 6; the experimental values are in line with the predicted values, and the relative errors are less than 5% from 3 independent experiments.

Table 6: Experimental verification results.

Serial number	Change rate of the cross-linking signal intensity		Yield of the recycled powder	
	Experimental value	Relative error	Experimental value	Relative error
1	31.723%	4.72%	88.743%	2.92%
2	32.276%	3.05%	89.198%	2.42%
3	32.034%	3.78%	88.275%	3.43%

5. Conclusion

(1) The highly active phenolic resin powder obtained by ultrafine pulverization of waste thermosetting phenolic resin sheet restores a certain ability to be reprocessed, and it was mixed with polyvinyl chloride at a ratio of 8 : 2 and molded. The tensile strength and bending strength of the recycled sheet can reach 8.13 MPa and 17.65 Mpa, respectively, which means that samples have good comprehensive mechanical properties.

(2) The stress field generated by the strong mechanical force acts on the molecular chain of the thermosetting phenolic resin, which caused the cross-linking bond of methylene bridge (-CH_2-) in the main chain and the methylol C-O bond on the branch to be broken, damaged highly cross-linking body network structure, reduced degree of cross-linking, and enhanced the activity of the recycled powder. The intensity of the cross-linking signal in the material continues to decrease with the decrease of the particle size, and it tends to be stable and stable at about 60% when the particle size exceeds 120 meshes.

(3) A quadratic regression model was established with the rotation speed, time, feed size, and feed volume as independent variables, the change rate of the cross-linking signal intensity, and the yield of the recycled powder as the response values, by using the Box-Behnken experimental design method. The influences on the change rate of the cross-linking signal intensity and the yield of the recycled powder are in orders: rotation speed, feed size, time, and feed volume. The best parameters for the thermosetting phenolic resin recovery are as follows: rotation speed of 2820 r/min, time of 80 min, feed particle diameter of 0.43 mm, and feed volume of 60 g.

Data Availability

The data used to support the findings of this study are included within the article.

Conflicts of Interest

The authors declare that there are no conflicts of interest regarding the publication of this paper.

Acknowledgments

This study was financially supported by the project of the National Natural Science Foundation of China (50975074), the Project of Natural Science Research of Colleges and Universities in Anhui Province, China (KJ2018A0456), and the Projects of Natural Science Research of Chaohu University, China (XLY-201703, XLY-201710).

References

[1] F. Bernardeau, D. Perrin, A.-S. Caro-Bretelle, J.-C. Benezet, and P. Ienny, "Development of a recycling solution for waste thermoset material: waste source study, comminution scheme and filler characterization," *Journal of Material Cycles and Waste Management*, vol. 20, no. 2, pp. 1320–1336, 2018.

[2] J. R. Correia, N. M. Almeida, and J. R. Figueira, "Recycling of FRP composites: reusing fine GFRP waste in concrete mixtures," *Journal of Cleaner Production*, vol. 19, no. 15, pp. 1745–1753, 2011.

[3] P. Asokan, M. Osmani, and A. D. F. Price, "Assessing the recycling potential of glass fibre reinforced plastic waste in concrete and cement composites," *Journal of Cleaner Production*, vol. 17, no. 9, pp. 821–829, 2009.

[4] A. J. Hulme and T. C. Goodhead, "Cost effective reprocessing of polyurethane by hot compression moulding," *Journal of Materials Processing Technology*, vol. 139, no. 1–3, pp. 322–326, 2003.

[5] P. Panyakapo and M. Panyakapo, "Reuse of thermosetting plastic waste for lightweight concrete," *Waste Management*, vol. 28, no. 9, pp. 1581–1588, 2008.

[6] H. S. Dweik, M. M. Ziara, and M. S. Hadidoun, "Enhancing concrete strength and thermal insulation using thermoset plastic waste," *International Journal of Polymeric Materials and Polymeric Biomaterials*, vol. 57, no. 7, pp. 635–656, 2008.

[7] J. Y. Guo, J. Guo, and Z. M. Xu, "Recycling of non-metallic fractions from waste printed circuit boards: a review," *Journal of Hazardous Materials*, vol. 168, no. 2-3, pp. 567–590, 2009.

[8] K. Nomaguchi and T. Nakagawa, "FRP recycling in EU, NA and pacific rim area-Challenging development in chemical recycling by subcritical water process," *Review of Automotive Engineering*, vol. 30, no. 1, pp. 3–10, 2009.

[9] S. J. Pickering, R. M. Kelly, J. R. Kennerley, C. D. Rudd, and N. J. Fenwick, "A fluidised-bed process for the recovery of glass fibres from scrap thermoset composites," *Composites Science and Technology*, vol. 60, no. 4, pp. 509–523, 2000.

[10] M. Modesti, A. Lorenzetti, F. Simioni, and G. Camino, "Expandable graphite as an intumescent flame retardant in polyisocyanurate-polyurethane foams," *Polymer Degradation and Stability*, vol. 77, no. 2, pp. 195–202, 2002.

[11] T. A. Turner, N. A. Warrior, and S. J. Pickering, "Development of high value moulding compounds from recycled carbon

fibres," *Plastics, Rubber and Composites*, vol. 39, no. 3–5, pp. 151–156, 2010.

[12] Y. Z. Zeng and C. J. You, "Advance in recycle of thermoset composites wastes," *Guangzhou Chemistry*, vol. 34, no. 2, pp. 54–60, 2009.

[13] Y. Tanaka, Q. Zhang, and F. Saito, "Mechanochemical dechlorination of chlorinated compounds," *Journal of Materials Science*, vol. 39, no. 16-17, pp. 5497–5501, 2003.

[14] K. Moribe, M. Tsuchiya, Y. Tozuka et al., "Grinding-induced equimolar complex formation between thiourea and ethenzamide," *Chemical & Pharmaceutical Bulletin*, vol. 52, no. 5, pp. 524–529, 2004.

[15] D. Yamaguchi, L. Maini, M. Polito et al., "Assembly of hybrid organic-organometallic materials through mechanochemical acid-base reactions," *Chemistry-A European Journal*, vol. 9, no. 18, pp. 4362–4370, 2003.

[16] Z. B. Mirolo, M. Wen, X. Y. Wang, Z. W. Zhang et al., "Lead mechanochemical sulfidation of fluorescent tube core glass," *China Environmental Science*, vol. 38, no. 11, pp. 4211–4217, 2018.

[17] L. Z. Xu, J. Zhang, Q. Sun, L. Q. Xu et al., "Surface modification of MSWI fly ash and its application in polypropylene composites," *Journal of Chemical Engineering of Chinese Universities*, vol. 32, no. 4, pp. 969–974, 2018.

[18] U. Heuert, M. Knörgen, H. Menge, G. Scheler, and H. Schneider, "New aspects of transversal 1H-NMR relaxation in natural rubber vulcanizates," *Polymer Bulletin*, vol. 37, no. 4, pp. 489–496, 1996.

[19] Y. F. Wang and C. G. Wang, "The application of response surface methodology," *Journal of the CUN*, vol. 14, no. 3, pp. 236–240, 2005.

[20] D. C. Montgomery, *Design and Analysis of Experiments*, China Statistics Press, Beijing, China, 1998.